Full Articles

The structures of the dicationic tetranitrosyl iron complex with cysteamine $[Fe_2S_2(CH_2CH_2NH_3)_2(NO)_4]^{2+}$ and its decomposition products in protic media: an experimental and theoretical study

N. S. Emelyanova,[a] A. F. Shestakov,[a] I. V. Sulimenkov,[b] T. N. Rudneva,[a] N. A. Sanina,[a] and S. M. Aldoshin[a]*

[a] *Institute of Problems of Chemical Physics, Russian Academy of Sciences, 1 prosp. Akad. Semenova, 142432 Chernogolovka, Moscow Region, Russian Federation. Fax: +7 (496) 522 3507. E-mail: n_emel@mail.ru*

[b] *Institute of Energy Problems of Chemical Physics, Chernogolovka Branch, Russian Academy of Sciences, 1 prosp. Akad. Semenova, 142432 Chernogolovka, Moscow Region, Russian Federation*

Decomposition products of $[Fe_2S_2(CH_2CH_2NH_3)_2(NO)_4]SO_4 \cdot 2.5H_2O$ (**1**′) were studied by electrochemistry and mass spectrometry. The structures of the dicationic tetranitrosyl iron complex with cysteamine of the composition $[Fe_2S_2(CH_2CH_2NH_3)_2(NO)_4]^{2+}$ (**1**) and possible products of its decomposition and NO replacement by an aqua ligand were studied by quantum chemical methods at the density functional theory level. Taking into account the solvation effects, the replacement of the nitrosyl ligand in dication **1** by an aqua ligand was found to be less favorable in aqueous solution than in the gas phase. The p*K* value was calculated for the proton abstraction from the NH_3 group of compound **1** (7.2), and the removal of NO from the deprotonated form of the complex was found to be much easier. This result is consistent with the experimental data on an increase in the rate of NO formation in aqueous solutions of **1** with increasing pH from 6 to 8 assuming that the increase in pH is accompanied by an increase in the percentage of the less stable deprotonated form of the complex and that OH^- does not participate in the elementary step of NO formation. The kinetic curves of NO formation are well described by a two-step scheme of consecutive first-order reactions of the NO formation and consumption. In the gas phase, dication **1** was found to be unstable to decomposition into two mononuclear cationic dinitrosyl iron complexes with cysteamine. This result is consistent with the fact that these cations are observed in the electrospray ionization mass spectrometric experiment. The major peak in the mass spectra is associated with the $[Fe_2S_2(CH_2CH_2NH_3)_2(NO)_4 - H]^+$ ion. As follows from the calculations, this is due to the deprotonation of the dication as it gets rid of the hydration shell, because even the dimer of water molecules is more basic than dication **1**.

Key words: NO donors, sulfur-nitrosyl iron complexes, mass spectrometry.

Numerous recent studies reliably established that NO plays a key role in various cellular functions, such as the blood pressure regulation, inhibition of platelet aggregation, immune cell response, antimicrobial activity, and so on.[1] These discoveries have stimulated great interest in biologically active metal complexes, particularly in those, which simulate the structures of nitrosyl cellular intermediates. Endogenous NO can be stabilized and stored in the form of dinitrosyl iron complexes (DNIC) with protein thiols, which extends its lifetime and retains its biological

Published in Russian in *Izvestiya Akademii Nauk. Seriya Khimicheskaya,* No. 1, pp. 1—11, January, 2012.

1066-5285/12/6101-1

activity.[2] According to ESR data, these non-heme iron nitrosyl complexes are $Fe(NO)_2$-type paramagnetic complexes, which are more well-known as complexes of "g = 2.03" family due to their characteristic isotropic g-factor.[3] A large series of compounds of the composition $Fe(NO)_2(L)_2$ (L ligands are derivatives of amino acids, peptides, or proteins) were discovered by ESR spectroscopy, in particular, in ferritin, which serves as the iron storage depot in the human body;[4] however, attempts to isolate these compounds failed. The main aim of the previous investigations was to detect these compounds because their isolation and study by direct structural methods present considerable difficulties. Dinitrosyl iron complexes are of particular interest because there is a limited assortment of synthetic analogs for investigations of the reactivity of DNIC, including processes of their formation in reactions of NO with iron-sulfur complexes and since DNIC exhibit pronounced biological (for example, antitumor[5]) activity. Hence, it is of interest to study the NO-donor activity and the mechanism of NO generation for the recently synthesized water-soluble dinuclear dicationic tetranitrosyl iron complex $[Fe_2S_2(CH_2CH_2NH_3)_2(NO)_4]SO_4 \cdot 2.5H_2O$ (**1**´).[6]

In the present study, we investigated the kinetics of NO accumulation in the course of hydrolysis of the dication $[Fe_2S_2(CH_2CH_2NH_3)_2(NO)_4]^{2+}$ (**1**) at different pH and performed a positive-ion electrospray ionization mass-spectrometric analysis of the complex. In addition, the electronic and molecular structures of dication **1**, as well as of those of possible products of its decomposition and replacement of NO by an aqua ligand, were studied by quantum chemical methods at the density functional theory level, which is extensively used nowadays to investigate the nature of iron-sulfur complexes with nitrosyl ligands.[7—13] Calculations were performed for the states with the lowest multiplicity (singlet and doublet), as well as for higher-multiplicity states (triplet and quartet), with the use of the GAUSSIAN (B3LYP method)[14] and PRIRODA (PBE method and the extended basis set for the SBK pseudopotential)[15] programs. Geometry optimization at the B3LYP level of theory was performed with the use of the 6-31G* basis set, and the energy was calculated using the 6-311++G** basis set with inclusion of the zero-point vibrational energy calculated with the 6-31G* basis set. The thermodynamic functions were determined using the harmonic oscillator—rigid rotator model. The characteristics of the electronic structures of the calculated complexes are presented in Table 1. In the calculations of the replacement and abstraction energies, the lowest-energy spin states obtained by the B3LYP method were taken into account. We failed to find states with the required open-shell electronic structure using the PRIRODA program. Hence, the energy data obtained at the PBE/SBK level of theory are less informative. However, it should be noted that calculations with the use of the PRIRODA program give more precise geometric characteristics, particularly, the bond lengths. On the whole, the difference in the valence distances estimated by two computational methods is at most 0.2 Å. The largest differences are observed for nonbonded Fe—Fe distances in the coordinatively unsaturated complexes.

Results and Discussion

The optimized geometry of the starting dication **1** (Fig. 1) in the singlet state agrees well with the experimental structural data.[6] The typical deviations of the bond lengths are no larger than 0.1 Å (B3LYP) and 0.03 Å (PBE); the deviations of the bond angles are no larger than 4°. The results of these calculations differ only slightly from the results of calculations at the BP86 level of theory with the use of the more extended TZVP basis set.[6]

As can be seen from Table 1, the solution with disturbed symmetry for the singlet state does not have a the correct spin structure, although the wave function satisfies the stability criterion. One unpaired electron is localized on each $Fe(NO)_2$ group. However, Fe atoms bear only about two instead of the expected three unpaired electrons, as in the case of triplet states with parallel spins of the $Fe(NO)_2$ fragments (see Table 1). This is also evident from the average squared spin values $\langle S^2 \rangle$ for the singlet

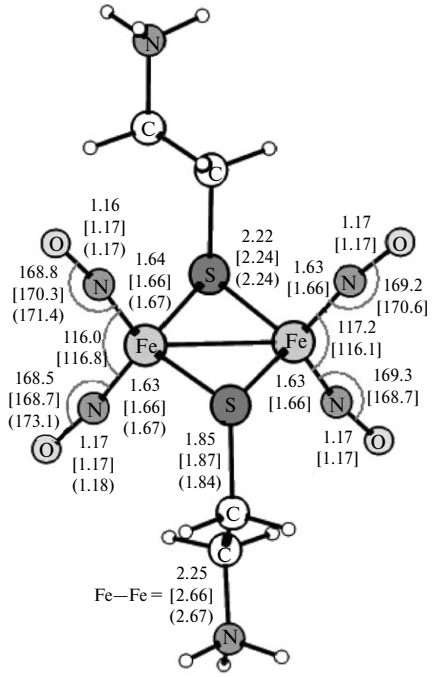

Fig. 1. Optimized geometric parameters of the starting dinuclear dication **1** calculated by the B3LYP/6-31G* and PBE/SBK (data in square brackets) methods. The experimental data for the starting complex are given in parentheses. Here and Figs 2—5, the distances are given in Å and the angles are given in degrees.

Table 1. Electronic characteristics of the starting dinuclear dication and its possible decomposition products

Complex	Multiplicity	E_{rel} /kcal mol^{-1}	Charge on the Fe atom	Spin density on NO	Charge on the S atom	Spin density on the S atom	Charge on the S atom	Spin density on the S atom	$<S^2>^a$ [$<S^2>$]^b
				B3LYP/6-311++G** calculations					
1a	1	0	0.44	±2.20	−0.25	−0.77	0.50	0.01	2.22 [9.25]
	1	7.7	0.54	2.00	−0.20	−0.69	0.57	0.03	1.39 [4.77]
			0.24	0.12	−0.32	—	0.44	—	—
1b	3	−22.4	0.89	3.21	−0.23	−1.18	−0.35	0.11	5.42 [14.25]
2a	2	0.6	0.91	±3.15	−0.27	−1.30[c]	−0.34	0.04	4.42 [14.53]
			0.62		−0.29	1.14	—	−0.02	—
					−0.24	—	—	—	—
2b	4	0	0.90	3.25	−0.37	−1.30[c]	−0.34	0.10	6.51 [10.36]
			0.72[c]		−0.18	−1.22	—	—	—
3a	2	−1.6	0.89	−3.20	−0.42[c]	−1.41[c]	−0.35	−0.04	4.61 [15.23]
			0.77[c]	3.30	0.25	1.19	—	—	—
					−0.20	1.13	—	—	—
3b	4	0	0.78[c]	3.32	−0.42[c]	−1.41	—	—	—
	−0.35	0.10	6.65	11.02	—	—	—	—	—
			0.90	3.22	−0.26	−1.19	—	—	—
					−0.20	−1.14	—	—	—
4a	1	19.1	0.88	±2.40	−0.52	0.97	0.27	0	2.70 [11.23]
					−0.28	0.81	0.34	—	—
4b	3	0	0.87	3.23	−0.29	−1.23	−0.32	0.12	5.49 [14.59]
					−0.22	−1.14	−0.38	—	—
5a	2	0	0.92	−3.15	−0.21	1.14	−0.36	—	—
	0.02	4.54	—	—	—	—	—	—	—
			0.65[c]	3.25[c]	−0.39[c]	1.15	−0.40	—	—
						−1.40[c]	—	—	—
				B3LYP/6-311++G** calculations					
5b	4	1.44	0.95	3.23	−0.22	−1.16	−0.41	0.10	6.60 [10.79]
			0.69[c]	3.30[c]	−0.40[c]	−1.14	—	—	—
						−1.42[c]	—	—	—
6a	2	−21.1	0.89	3.24	−0.19	−1.12	−0.29	0.08	2.47 [4.71]
					−0.22	—	—	—	—
6b	4	0	0.87	3.26	−0.24	−0.99	−0.26	0.08	4.54 [4.01]
					−0.17	0.64	—	—	—
7a	2	0	0.94	3.25	−0.27	−1.16	−0.37	0.08	2.54 [5.08]
					−0.23	−1.18	—	—	—
7b	4	20.3	0.95	3.37	−0.27	−1.14	−0.38	0.07	4.78 [4.24]
					−0.21	0.65	—	—	—
8a	1	0	0.42	−0.68	−0.14	0.76	−0.17	−0.06	1.29 [2.18]
8b	3	−24.2	0.64	3.25	−0.20	−1.28	−0.27	0.02	3.02 [2.51]
9a	1	0	0.20	−0.96	−0.30	0.89	0.12	0.07	1.02 [1.57]
9b	3	−27.9	0.75	3.27	−0.43	−1.43	−0.27	0.09	3.12 [2.60]
10a	1	0	0.21	1.04	−0.29	−1.00	0.17	−0.01	0.80 [1.08]
10b	3	−27.2	0.79	3.27	−0.40	−1.30	−0.44	0.05	3.14 [2.63]
				PBE/SBK calculations					
1a	1	0	0.57		−0.25	—	−0.01	—	—
					−0.18	—	0.03	—	—
1b	3	15.1	0.71	1.70	−0.24	−0.41	−0.07	0.15	—
					−0.18	—	−0.09	0.12	—
2a	2	0	0.68[c]	1.98[c]	−0.26[c]	−0.51[c]	−0.08	−0.04	—
			0.55	−0.79	−0.23	0.19	—	—	—
2b	4	6.7	0.63	2.81[c]	−0.20[c]	−0.60[c]	−0.08	0.11	—
				1.09	−0.22	−0.31	−0.12	0.12	—
						−0.24	—	—	—

(*to be continued*)

Table 1 (*continued*)

Complex	Multiplicity	E_{rel} /kcal mol^{-1}	Charge on the Fe atom	Spin density on NO	Charge on the S atom	Spin density on the S atom	Charge on the S atom	Spin density on the S atom	$<S^2>^a$ $[<S^2>]^b$
				PBE/SBK calculations					
3a	2	0	0.80[c]	1.88[c]	−0.47[c]	−0.51[c]	−0.08	−0.02	—
			0.52	−0.78	−0.24	0.20	—	—	—
					−0.22	—	—	—	—
3b	4	−0.17	0.77[c]	2.79[c]	−0.31[c]	−0.62[c]	−0.07	0.15	—
			0.69	1.00	−0.41	−0.25	−0.13	0.16	—
					−0.32	—	—	—	—
4a	1	0	0.61		−0.26	—	0	—	—
					−0.16	—	—	—	—
4b	3	18.1	0.61		−0.27	—	0	—	—
					−0.17	—	—	—	—
5a	2	0	0.70[c]	1.80[c]	−0.33[c]	−0.41[c]	−0.11	0.11	—
			0.54	−0.68	−0.24	0.17	—	—	—
					−0.16	0.17	—	—	—
5b	4	7.8	0.67[c]	2.78[c]	−0.39[c]	−0.62[c]	−0.01	0.13	—
			0.67	1.04	−0.46	−0.24	—	—	—
					−0.19	−0.27	—	—	—
6a	2	0	0.78	1.82	−0.30	−0.48	−0.12	0.13	—
					−0.16	−0.45	—	—	—
6b	4	−48.9	0.79	2.43	−0.29	0.18	−0.09	0.25	—
					−0.20	0.13	—	—	—
7a	2	0	0.78	1.84	−0.33	−0.50	−0.19	0.14	—
					−0.15	—	—	—	—
7b	4	24.44	0.80	2.28	−0.36	0.29	−0.17	0.16	—
					−0.15	0.25	—	—	—
8a	1	0	0.58		−0.32	—	−0.05	—	—
8b	3	22.9	0.49	2.64	−0.13	−0.72	−0.11	0.09	—
9a	1	0	0.78		−0.50	—	−0.18	—	—
9b	3	−15.71	0.83	2.45	−0.50	−0.65	−0.20	0.18	—
10a	1	0	0.74		−0.46	—	−0.27	—	—
10b	3	−13.22	0.82	2.58	−0.42	−0.71	−0.34	0.09	—

[a] The average square of the spin.
[b] The average squared spin value after annihilation of the wave function term with the spin one unit larger than the starting one.
[c] Characteristics of the coordination site with one NO group.

state with broken symmetry (2.22). In the case of the correct spin structure, this value should be close to 5.[16] For the triplet state, $<S^2> = 5.42$, which is rather close to the theoretical value of 6.[16] Hence, the triplet state of the complex with an elongated Fe—Fe distance (3.37 Å (B3LYP) and 3.02 Å (PBE)) lies 22.4 kcal mol^{-1} lower on the energy scale. Attempts to find the singlet solution with broken symmetry and correct spin structure by varying the initial approximation to the wave function failed. We found only one additional higher-lying singlet state with even smaller $<S^2> = 1.39$ and a nonuniform spin distribution over the Fe atoms (see Table 1). This creates some difficulties in the consideration of the energy difference between the zero and non-zero spin states, because this value has a contribution of an nonphysical change in the electronic structures of the Fe atoms and NO ligands. Hence, to minimize this systematic error, we performed calculations with the use of the energies of the complex in the triplet state.

Release of NO from the starting complex. The simplest mechanism of nitric oxide release followed by coordination of an aqua ligand to the free coordination site (Fig. 2) was considered as the generation reaction of NO. The doublet and quartet states of the complex $[Fe_2(SCH_2CH_2NH_3)_2(NO)_3]^{2+}$ (**2**) obtained after the NO elimination from the starting dinuclear complex are virtually degenerate. This is an open-shell complex and the values $<S^2> = 4.42$ and 6.51 are quite close to the theoretical values[16] for the doublet and quartet states (4.75 and 6.75, respectively). Good agreement was also obtained for other calculated dinuclear and mononuclear open-shell complexes. Noteworthy is the formation of a hydrogen bond (1.97 Å) between a proton of the NH_3 group of the

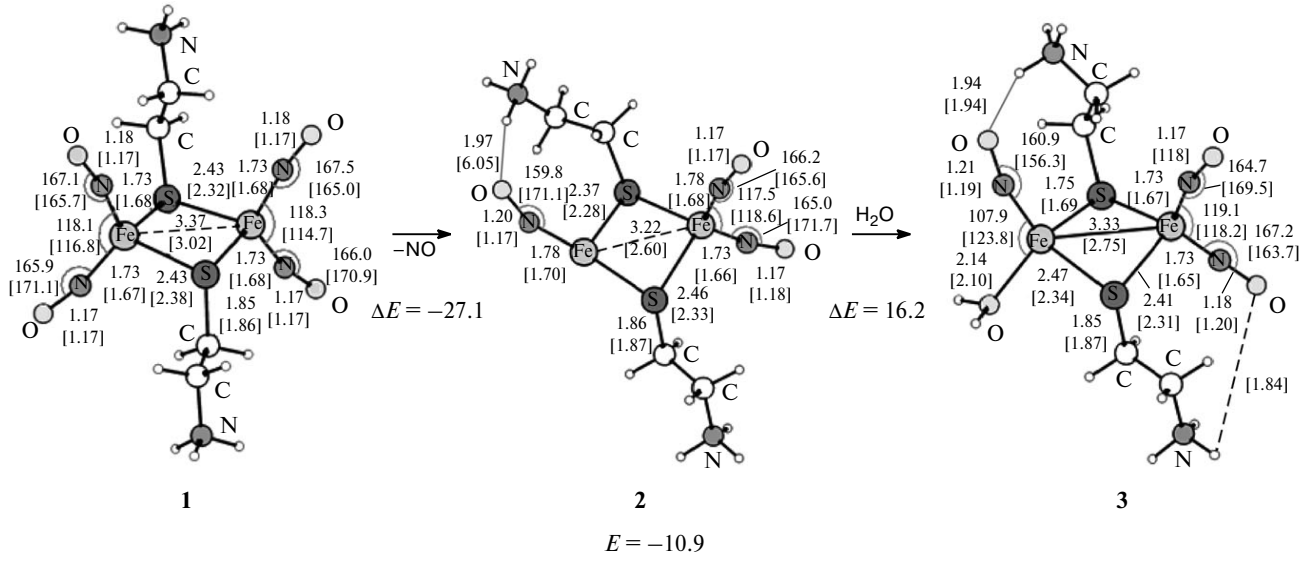

Fig. 2. Replacement of NO by an aqua ligand in the dinuclear cation. Calculated by the B3LYP/6-31G* and PBE/SBK (data in square brackets) methods. Here and Figs 3—5, the energy is given in kcal mol^{-1}.

cysteamine ligand and the oxygen atom of a single NO group. This leads to a substantial distortion of the structure and is associated with an increase in the negative charge on the oxygen atom (see Table 1). The calculated Fe—NO bond energy is 27.1 kcal mol^{-1}, which is close to the value found for a similar neutral dinuclear sulfur-nitrosyl iron complex (29.2 kcal mol^{-1}).[17]

The energies of the doublet and quartet states of the complex with an aqua ligand $[Fe_2S_2(CH_2CH_2NH_3)_2(NO)_3(H_2O)]^{2+}$ (**3**) are also virtually equal to each other. Due to the donor properties of the H_2O molecule, the negative charge on the oxygen atom of the adjacent NO group substantially increases. This leads to a shortening of NH_3...ON hydrogen bonds accompanied by a slight increase in the Fe—NO distance compared to the coordinatively unsaturated complex. The calculated bond energy of the aqua ligand is 16.2 kcal mol^{-1}. On the whole, the replacement of NO by an aqua ligand in the dinuclear iron-sulfur complex with the cysteamine ligand requires an energy of 10.9 kcal mol^{-1}. Therefore, on the one hand, the complex is quite stable to the Fe—NO bond dissociation (this is consistent with the experimental data); on the other hand, the NO group can be eliminated by the replacement with an aqua ligand.

Release of NO from the deprotonated complex. Deprotonation of the cysteamine ligand in complex **1** (Fig. 3)

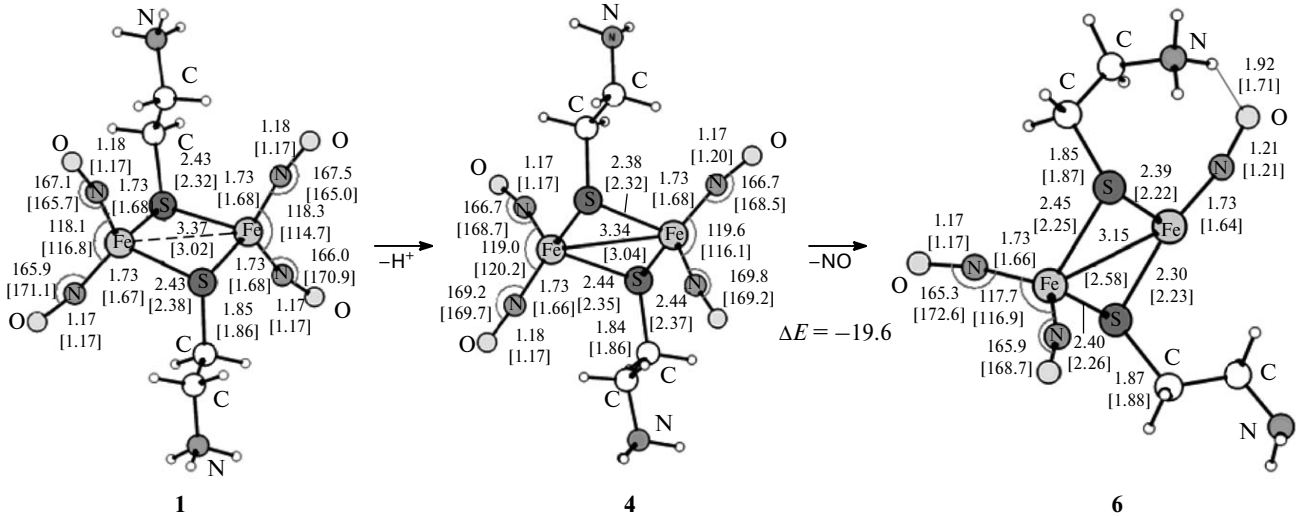

Fig. 3. Abstraction of a proton from the dinuclear dication to form the dinuclear monocation followed by NO release. Obtained from B3LYP/6-31G* and PBE/SBK (data in square brackets) calculations.

requires an energy of 172.6 kcal mol^{-1} (7.41 eV). This value can be related to the proton affinity of a water molecule (7.06 and 7.16 eV according to B3LYP and PBE calculations, respectively; the experimental value is 7.14 eV). Hence, although the basicity of the nitrogen atom in the cysteamine ligand decreases due to the positive charge of the complex, it is still higher than the basicity of a water molecule in the gas phase. However, the most stable structures of the hydrated proton include at least two water molecules. The proton affinity of two water molecules is 8.59 (B3LYP) and 8.23 eV (PBE). Hence, it would be expected that proton abstraction from the complex $[Fe_2(SCH_2CH_2NH_3)_2(NO)_3]^{2+}$ (**2**) by a water dimer to form the monocation is thermodynamically favorable in the gas phase.

In deprotonated complex **4**, the energy of the N—O bond in the ligand substantially decreases to 19.6 kcal mol^{-1}. This may be associated with two factors. First, the Fe—NO bond lengths in the deprotonated complex are somewhat larger than in the starting complex. Second, due to the lower positive charge in the complex formed after the elimination of NO, the Fe atoms have stronger donor properties. This leads to a shortening of the intramolecular hydrogen bonds between the NO ligand and the NH_3 group (see Fig. 3). This effect is similar in magnitude to the effect of coordination of a water molecule.

Dissociation of dinuclear complex. Dinuclear sulfur-nitrosyl iron clusters can dissociate into mononuclear complexes under certain conditions.[18] Hence, we considered the decomposition of isolated complex **1** into two cationic three-coordinate iron complexes **6** (Fig. 4). This process is accompanied by an energy gain of 8.3 kcal mol^{-1}. This is indicative of a considerable contribution of the Coulomb repulsion, which is larger than the total energy of Fe—S coordination bonds.

The addition of a water molecule to the coordination vacancy affords mononuclear complex **7** with an energy gain of 25.6 kcal mol^{-1}. In this complex, the iron atom is in tetrahedral coordination; the Fe—N and N—O distances are virtually equal to those in the corresponding complexes **1** and **3**. The energy of the doublet state of complex **7** is lower than that of the quartet state. Therefore, the total energy gain upon dissociation of the dinuclear complex accompanied by the addition of two water

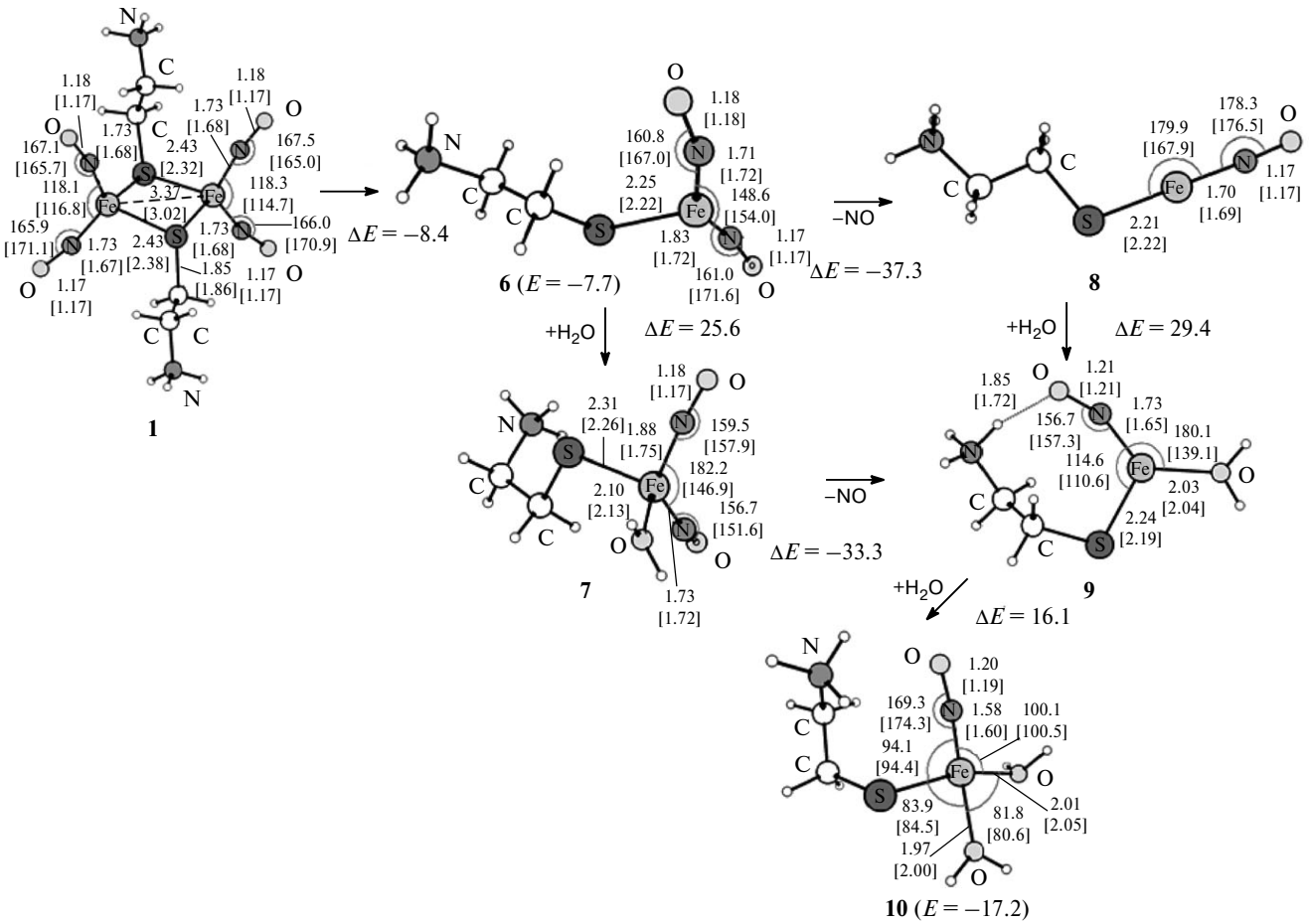

Fig. 4. Decomposition of the dinuclear dication into mononuclear cations and the reactions in them. Calculated by the B3LYP/6-31G* and PBE/SBK (data in square brackets) methods.

molecules is 59.5 kcal mol^{-1}. For the mononuclear complex **7**, the NO release energy is 33.3 kcal mol^{-1}, which is somewhat higher than for the dinuclear complex. The release of NO from complex **6** results in complex **8** and requires an energy of 37.3 kcal mol^{-1}. Like the replacement of the nitrosyl ligand by an aqua ligand, the latter process is accompanied by an increase in the energy by 7.7 kcal mol^{-1}.

In the coordinatively unsaturated complex $Fe(SCH_2CH_2NH_3)(NO)(H_2O)]^+$ (**9**), the negative charge on the O atom of the NO ligand also increases, resulting in the formation of an intramolecular hydrogen bond. The incorporation of the second water molecule into the coordination sphere of complex **9** is accompanied by a slight energy gain (16.1 kcal mol^{-1}) and leads to structure **10**. As follows from these data, the replacement of NO by an aqua ligand in mononuclear complex **7** requires an energy of 17.2 kcal mol^{-1}, which is also slightly larger than in the case of the dinuclear complex.

Influence of solvation effects. The thermodynamic characteristics of the decomposition of the dinuclear iron-sulfur complex with cysteamine resulting in the release of NO in aqueous solution were calculated taking into account the solvation effects using the polarized continuum model (Table 2) (B3LYP, 6-311++G** basis set). In this case, the energy of the replacement of the nitrosyl ligand by an aqua ligand in dinuclear dication **1** increases to 22 kcal mol^{-1} (*cf.* an almost equal energy of 21 kcal mol^{-1} for mononuclear cation **7**). This increase in the energy of replacement in aqueous solution compared to the gas phase is associated with the 10 kcal mol^{-1} difference between the solvation energies of water and nitric oxide. In aqueous solution, the solvation energies of coordinatively saturated and unsaturated complexes are also substantially different, and, consequently, the energy of NO release from the dinuclear complex in water is half the gas-phase value (11.6 kcal mol^{-1}), whereas the addition of water requires an energy expenditure of 10.4 kcal mol^{-1}. The removal of the nitrosyl ligand from mononuclear complex **7** in solution requires an energy of 15.4 kcal mol^{-1}, which is also approximately two times smaller than that in the gas phase, and the addition of water is accompanied by an increase in the energy by 5.6 kcal mol^{-1}. The dissociation of dication **1** into two monocations **5** in aqueous solution requires a small energy (only 6.2 kcal mol^{-1}), which also makes this process feasible. Taking into account the addition of water molecules to coordinatively unsaturated mononuclear complexes **5**, we obtain:

$$\underset{\mathbf{1}}{[Fe_2S_2(CH_2CH_2NH_3)_2(NO)_4]^{2+}} + 2\,H_2O = 2\,[Fe(SCH_2CH_2NH_3)(NO)_2(H_2O)]^+ . \quad (1)$$

The decomposition becomes energetically favorable. However, due to the entropy loss in the reaction (1), the total change in the Gibbs free energy is close to zero, and the corresponding equilibrium constant is 16. As a result, mono- and dinuclear iron nitrosyl complexes would be expected to coexist in solution. However, taking into account the energies of NO elimination, the former complexes are more stable. In addition, reaction (1) is accompanied by the cleavage of two Fe—S bonds and is not an elementary step but involves several steps (Fig. 5) with activation barriers. Hence, an induction period would be expected before the establishment of the equilibrium in solution.

Table 2. Energies of the reaction (E_r) taking into account the solvation effect in terms of the polarized continuum model

Reaction	$-E_r$/kcal mol^{-1}	
	Dinuclear dication	Mononuclear cation
Replacement of NO by an aqua ligand	22.1	21.2
Release of NO	11.6	15.4
Addition of H_2O	10.4	5.6
Decomposition	6.2	—

Taking into account the solvation effects, the deprotonation of cation **1** requires a slight increase in the Gibbs free energy (by 7.2 kcal mol^{-1}), which corresponds to pK 7.2. Therefore, one can expect that in a weakly alkaline medium, the equilibrium will be shifted toward the monocation in water.

The kinetics of NO formation in solution. We studied the NO-donor activity of complex **1′** in aqueous solutions at three different pH values (Fig. 6) using a NO-selective amperometric electrode. As can be seen from Fig. 6, the acidity of the medium substantially affects both the initial rate of NO formation and the maximum concentration of NO generated. The inset (see Fig. 6) shows that the NO concentration linearly depends on the time during the first 50 s, after which the curves reach a plateau with the following maximum [NO] values: ~25, ~50, and ~220 nmol L^{-1} at pH = 6, 7, and 8, respectively. A small induction period was ignored.

At pH = 8, the kinetic curve shows a pronounced maximum. This fact unambiguously indicates that NO is an intermediate and that a substantial difference between the maximum NO yield and the stoichiometric value equal to unity is due to some secondary reactions with the participation of NO. The simplest two-step scheme proposed in our previous study[16] involves the following two consecutive irreversible reactions:

$$LFe(NO) \xrightarrow{k_1} LFe + NO,$$

$$NO \xrightarrow{k_2} P,$$

where L = $[Fe(\mu_2\text{-}SR)_2(NO)_3]$ and P are products.

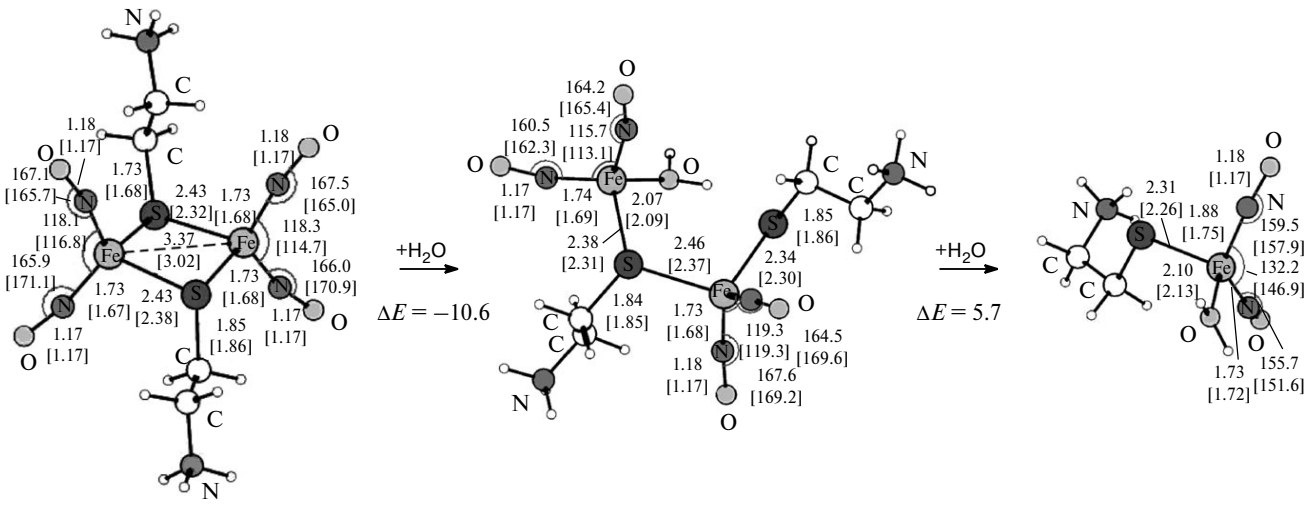

Fig. 5. Decomposition of the dinuclear dication under the action of H_2O molecules according to B3LYP/6-31G* and PBE/SBK (data in square brackets) calculations. The energies were calculated taking into account the solvation effects in terms of the polarized continuum model.

This scheme efficiently takes into account the formation and consumption of NO and gives the following dependence of the NO concentration on time:

$$[NO] = [Ck_1/(k_2 - k_1)][\exp(-k_1 t) - \exp(-k_2 t)],$$

which has a maximum at $t = (\ln k_1 - \ln k_2)/(k_1 - k_2)$.

This scheme was used to describe the kinetic curves. The C, k_1, and k_2 values estimated from the experimental data by the least-squares method are given in Table 3. As can be seen from Fig. 6, the resulting analytical dependence describes the experimental data with good accuracy. Based on analysis of the results, the following conclusions can be drawn. First, the hydroxyl ion, which could be incorporated instead of the eliminated NO molecule, is not involved in the rate-limiting step; otherwise, the effective rate constant k_1 would be proportional to the OH^- concentration. According to the experimental data, the kinetic curves of NO release at pH 6 and 7 are close to each other, and a sharp increase in the decomposition of the complexes accompanied by the NO release is observed only at pH 8. Hence, we attribute the increase in the rate of NO formation to the fact that in alkaline media, the concentration of the deprotonated complex that is formed in the reaction with the base is higher

$$[Fe_2(SCH_2CH_2NH_3)_2(NO)_4]^{2+} + OH^- \rightleftharpoons$$

$$\rightleftharpoons [Fe_2(SCH_2CH_2NH_3)(SCH_2CH_2NH_2)(NO)_4]^{+} + H_2O. \quad (2)$$

According to theoretical estimates, this complex contains a more weakly bound NO molecule compared to the starting complex. Taking into account the calculated pK value for complex **1**, it would be expected that the equilibrium in reaction (2) will be completely shifted to the right at pH > 7.2. Since the protolytic equilibria are fast reac-

Table 3. Parameters describing the kinetic curves (see Fig. 5) at different pH

pH	C /mol of NO (mol of **1**)$^{-1}$	k_1	k_2
		s^{-1}	
6.0	$0.008\pm1.2\cdot10^{-5}$	0.01696±0.00006	$0.00041\pm4\cdot10^{-6}$
7.0	$0.015\pm2.4\cdot10^{-5}$	0.01706±0.00007	$0\div4.6628\cdot10^{-6}$
8.0	0.29±0.036	0.00342±0.00009	0.00214±0.00007

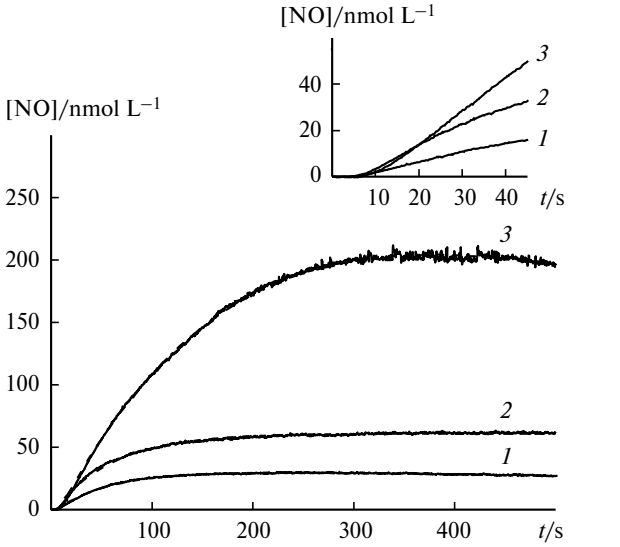

Fig. 6. Time dependences of the concentration of NO generated by complex **1**′ in aqueous aerobic solutions at pH 6.0 (*1*), 7.0 (*2*), and 8.0 (*3*) at $T = 25$ °C.

Table 4. Mass spectrometric data for a solution of complex **1** in H_2O ($2.7 \cdot 10^{-3}$ mol L^{-1})

Ion	*m/z*	I_{rel}* at different *t*/min				
		3	6	39	87	133
$[Fe(S(CH_2)_2NH_3)(NO)_2]^+$ (**6**)	192.97	0.002	0.003	0.002	0.002	0.0015
$[Fe_2(S(CH_2)_2NH_3)_2(NO)_4 - 2\,H - 2\,NO]^+$	323.92	0.010	0.014	0.009	0.009	0.0060
$[Fe_2(S(CH_2)_2NH_3)_2(NO)_4 - H - NO]^+$	354.93	0.019	0.022	0.019	0.018	0.0130
$[Fe_2(S(CH_2)_2NH_3)_2(NO)_4 - H]^+$ (**4**)	384.93	1.000	1.000	1.000	1.000	1.0000
		(37314)	(38709)	(37708)	(37511)	(36553)

* Relative intensities of ion peaks and the absolute amounts of the $[Fe_2(S(CH_2)_2NH_3)_2(NO)_4 - H]^+$ ions (in parentheses) in 200000 accumulation cycles (within 40 s).

tions, the equilibrium concentrations of the deprotonated complex **4** will be determined exclusively by the pH value. The rate of NO formation will increase with increasing concentration of complex **4**. This conclusion is consistent with the experimental observations on the threshold increase in the rate of NO generation as pH increases from 6 to 8.

Mass spectrometric measurements. To study the ion dynamics in the aqueous solution of complex **1´**, we recorded the mass spectra of solutions of **1´** within 3, 6, 39, 87, and 133 min after their preparation (Table 4, see Fig. 6) at pH 6.5. All detected major ions were identified based on the analysis of the isotopic distributions of the ion peaks and measurements of exact ion masses.

The results of the processing of the mass spectra are presented in Table 4. The experimental mass to charge ratios (*m/z*) for the peaks corresponding to the major isotopes are given. The relative intensity of the ions equal to unity signifies that the amount of these ions in the recorded mass spectrum is the largest one; the intensities of other ions in the spectrum are normalized to the maximum value. Table 4 also gives the absolute amounts of the major $[Fe_2(S(CH_2)_2NH_3)_2(NO)_4 - H]^+$ ions in 200 000 accumulation cycles (within 40 s). The relative intensities of the ions, which are decomposition products of complex **1´**, are not higher than 2.2%. A slight increase in the relative intensities of the ion peaks corresponding to the products at $t = 6$ min followed by a decrease at $t = 133$ min are observed.

The isotopic distribution with the maximum intensity (Fig. 7, *a*) corresponds to the $[Fe_2(S(CH_2)_2NH_3)_2(NO)_4 - H]^+$ ions. It should be noted that the peak of the starting complex is not detected at all, and the spectrum shows only the peak of the mononuclear complex $[Fe(S(CH_2)_2NH_3)(NO)_2]^+$. The nature of the major peak in the mass spectra corresponds to the results of theoretical calculations, according to which the proton transfer from the dication to the water dimer is energetically favorable. This reaction occurs as the positively charged complex gets rid of the hydration shell in the electrospray ionization mass spectrometric experiment. An alternative dissociation of the dication into two monocations $[Fe(S(CH_2)_2NH_3)(NO)_2]^+$ is also thermodynamically favorable in the gas phase. However, a high activation energy would be expected for this process due to the simultaneous cleavage of two Fe—S bonds. Hence, this process is slower, which explains the smaller percentage of these cations in the mass spectra. As can be seen from Fig. 7, *b*, the amount of $[Fe_2(S(CH_2)_2NH_3)_2(NO)_4 - H]^+$ ions in the mass spectrum recorded after 130 min remains virtually unchanged (the difference is less than 1%). Based on these data and on the analysis described above, it can be concluded that the concentration of complex **4** in the solution under consideration remains approximately constant for at least 2 h. Since the concentration of complex **1** in the electrospray ionization mass spectrometric experiments

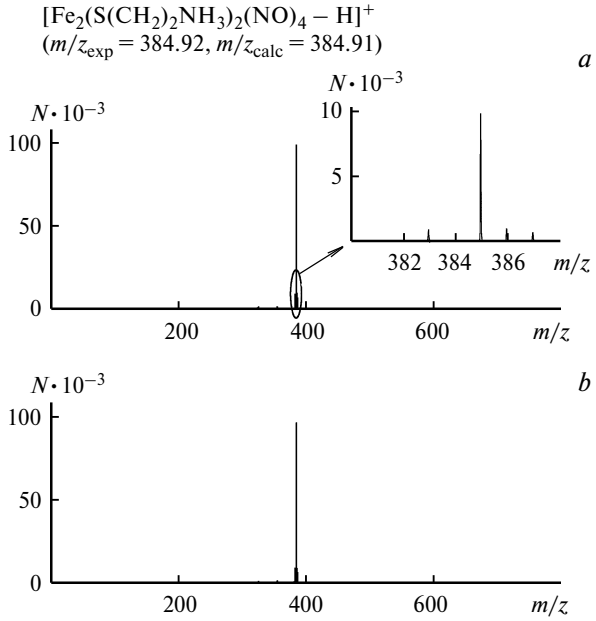

Fig. 7. Mass spectra of an aqueous solution of complex **1´** ($2.7 \cdot 10^{-3}$ mol L^{-1}) recorded 3 (*a*) and 133 min after the preparation of the solution (*b*); *N* is the number of ions. Inset: detailed isotopic distribution corresponding to $[Fe_2(S(CH_2)_2NH_3)_2(NO)_4 - H]^+$ ions.

was several orders of magnitude higher than in the electrochemical experiment, the results can be compared only very roughly. It should be noted that the constancy of the signal of the major peak qualitatively corresponds to the kinetic data (see Fig. 6) at pH < 6 and 7, from which it follows that the yield of NO based on complex **1** is only a few percentage.

Due to both processes, the concentration of the starting complex in the gas phase becomes negligible.

The factors responsible for the appearance of the peak of the $[Fe_2(S(CH_2)_2NH_3)_2(NO)_4 - 2\,H - 2\,NO]^+$ ion due to the elimination of the nitroxyl HNO from the denitrosylated monocation $[Fe_2(S(CH_2)_2NH_3)_2(NO)_4 - H - NO]^+$ remain unclear. Apparently, this is associated with the formation of intramolecular hydrogen bonds with the participation of the NO ligand in denitrosylated complexes (see structures **2**, **3**, and **9** in Figs 2—4).

According to experimental data and to the results of quantum chemical calculations, the dicationic complex $[Fe_2S_2(CH_2CH_2NH_3)_2(NO)_4]^{2+}$ (**1**) is unstable to dissociation into two monocations in the gas phase but is dissociation-stable in aqueous medium. In the gas phase, two water molecules are sufficient for the deprotonation. Hence, the major peak in the mass spectra is associated with the $[Fe_2S_2(CH_2CH_2NH_3)_2(NO)_4 - H]^+$ ion. In an aqueous solution, replacement of the nitrosyl ligand by an aqua ligand is less favorable than in the gas phase; however, the elimination of NO from the mononuclear cation and the dinuclear dication of sulfur-nitrosyl iron complexes occur more easily. Since the NO ligand in the mononuclear complexes is bound stronger than in the dinuclear complexes, the formation of NO in aqueous solutions, apparently, occurs through the decomposition of the starting dinuclear complexes rather than the secondary mononuclear complexes. In the deprotonated dinuclear complexes, the N—O bond energy of the ligand substantially decreases compared to the starting complexes. The deprotonation of this complex in water requires a low energy, which is responsible for the experimentally observed increase in the rate of NO generation at pH > 7. The kinetic curves of NO formation are well described by a two-step scheme of first-order reactions of the NO formation and consumption. The observed constants for this kinetic scheme are consistent with the mechanism of the predominant formation of NO from the deprotonated dinuclear complexes.

The mechanism of hydrolysis of sulfur-nitrosyl iron complexes calls for further investigation. It is known[14] that the redox behavior of NO in aqueous solutions strongly depends not only on the pH of the medium but also on the concentration of molecular oxygen in the system under study. Hence, the contributions of other processes, in which molecular oxygen directly interacts with the complex under consideration or promotes the formation of long-lived nitrosyl intermediates, cannot be ruled out. Nevertheless, taking into account the theoretical data, one can expect that the effect of the pH of the medium on the rate of NO generation under anaerobic conditions is determined by an increase in the concentration of the less stable deprotonated complex. This is a very interesting fact because prerequisites for the local generation of large amounts of NO in regions with low acidity are thus created. Hence, iron nitrosyl complexes characterized by the strong pH dependence of their NO-donor activity may be of particular interest for practical applications as drugs.

Experimental

Polycrystals of **1**´ were synthesized according to a procedure described previously.[6]

Quantum chemical calculations were performed by the B3LYP method using the GAUSSIAN 98 program.[14] Geometry optimization was carried out with the 6-31G* basis set. The energy was calculated using the 6-311++G** basis set with inclusion of the zero-point vibrational energy calculated with the 6-31G* basis set. The calculations were performed with the use of the GAUSSIAN program (B3LYP method, 6-31G* basis set (for geometry optimization) and 6-311G** basis set (for energy calculations)) and the PRIRODA program (PBE functional, SBK basis set).[15]

Electrochemical determination of NO. The concentration of NO generated by complex **1** in aqueous solutions with different acidity was measured using an amiNO-700 sensor electrode of the inNO Nitric Oxide Measuring System (Innovative Instruments, Inc., USA). The NO concentration was detected at 0.2 s intervals during 500 s in buffer solutions containing complex **1** at a concentration of $0.4 \cdot 10^{-5}$ mol L^{-1}. The electrochemical sensor was calibrated using a 100 μM aqueous $NaNO_2$ reference solution, to which a mixture of KI (Aldrich) (20 mg), 1 M H_2SO_4 (2 mL), and water (18 mL) was added.[19] All experiments were performed in a temperature-controlled cell at 25 °C with vigorous stirring. A phosphate buffer, pH 7.0 (Hydrion^{TM}, Aldrich) were used. The buffers, pH 6 and 8, were prepared from 0.3 M K_2HPO_4 and KH_2PO_4 solutions according to a procedure described previously,[20] The pH values of the solutions were measured using an HI 8314 membrane pH-meter (HANNA Instruments, Germany).

Mass spectra of aqueous solutions of complex **1** were obtained on a high-resolution orthogonal-injection time-of-flight mass spectrometer.[21] The ions were extracted from the samples using an atmospheric electrospray ionization source without forced supply of the solution (flow rate was 0.1 μL min^{-1}, the inner diameter of the quartz capillary was 50 μm, the voltage between the capillary and the inlet of the mass spectrometer was ~3 kV). The concentration of complex **1** was 2.7 mmol L^{-1} at pH 6.5. Pure nitrogen at room temperature was used as the buffer gas. The voltage between the inlet of the mass spectrometer and the skimmer was maintained at 50 V to minimize the fragmentation in this region. The spectral resolution of the time-of-flight mass spectrometer was ~8000. The accuracy of the determination of the ion mass was 20 ppm.

This study was financially supported by the Presidium of the Russian Academy of Sciences (Program "Basic Sci-

ences for Medicine") and the Russian Foundation for Basic Research (Project No. 09-03-12036-m).

References

1. *Nitric Oxide: Biology and Pathobiology*, Ed. L. J. Ignarro, Academic Press, San Diego, 2000.
2. R. J. Dai, S. C. Ke, *J. Phys. Chem. B*, 2007, **111**, 2335.
3. A. F. Vanin, *Nitric Oxide*, 2009, **21**, 1.
4. L. Li, *Commun. Inorg. Chem.*, 2002, **23**, 335.
5. N. A. Sanina, O. S. Zhukova, Z. S. Smirnova, L. M. Borisova, M. P. Kiseleva, S. M. Aldoshin, *Ross. Bioterapevt. Zh.* [*Russ. Biotherap. J.*], 2008, No. 1, 52 (in Russian).
6. T. N. Rudneva, N. A. Sanina, K. A. Lysenko, S. M. Aldoshin, M. Y. Antipin, N. S. Ovanesyan, *Mendeleev Commun.*, 2009, **19**, 253.
7. L. Li, R. Wang, M. A. Camacho-Fernandez, W. Xu, J. Zhang, *J. Biol. Inorg. Chem.*, 2009, **14** (Suppl.), S132.
8. M. Li, D. Bonnet, E. Bill, F. Neese, T. Weyhemuller, N. Blum, D. Sellmann, K. Weghardt, *Inorg. Chem.*, 2002, **41**, 3444.
9. J. Conradie, D. A. Quarless, Jr., H-F. Hsu, T. C. Harrop, S. J. Lippard, S. A. Koch, A. Ghosh, *J. Am. Chem. Soc.*, 2007, **128**, 10446.
10. E. Tangen, J. Conradie, A. Ghosh, *Inorg. Chem.*, 2005, **44**, 8699.
11. I.-J. Hsu, C.-H. Hsieh, S.-C. Ke, K.-A. Chiang, J.-M. Lee, J.-M. Chen, L.-Y. Jang, G.-H. Lee, Y. Wang, W.-F. Liaw, *J. Am. Chem. Soc.*, 2007, **129**, 1151.
12. S. Ye, F. Neese, *J. Am. Chem. Soc.*, 2010, **132**, 3646.
13. K. H. Hopmann, J. Conradie, A. Ghosh, *J. Phys. Chem., B*, 2009, **113**, 10540.
14. M. J. Frisch, G. W. Trucks, H. B. Schlegel, G. E. Scuseria, M. A. Robb, J. R. Cheeseman, V. G. Zakrzewski, J. A. Montgomery, Jr., R. E. Stratmann, J. C. Burant, S. Dapprich, J. M. Millam, A. D. Daniels, K. N. Kudin, M. C. Strain, O. Farkas, J. Tomasi, V. Barone, M. Cossi, R. Cammi, B. Mennucci, C. Pomelli, C. Adamo, S. Clifford, J. Ochterski, G. A. Petersson, P. Y. Ayala, Q. Cui, K. Morokuma, D. K. Malick, A. D. Rabuck, K. Raghavachari, J. B. Foresman, J. Cioslowski, J. V. Ortiz, A. G. Baboul, B. B. Stefanov, G. Liu, A. Liashenko, P. Piskorz, I. Komaromi, R. Gomperts, R. L. Martin, D. J. Fox, T. Keith, M. A. Al-Laham, C. Y. Peng, A. Nanayakkara, C. Gonzalez, M. Challacombe, P. M. W. Gill, B. Johnson, W. Chen, M. W. Wong, J. L. Andres, C. Gonzalez, M. Head-Gordon, E. S. Replogle, J. A. Pople, *Gaussian 98, Revision A.7*, GAUSSIAN, Inc., Pittsburgh (PA), 1998.
15. D. N. Laikov, *Chem. Phys. Lett.*, 1997, **281**, 151.
16. N. A. Sanina, G. V. Shilov, S. M. Aldoshin, A. F. Shestakov, L. A. Syrtsova, N. S. Ovanesyan, E. S. Chudinova, N. I. Shkondina, N. S. Emel´yanova, A. I. Kotel´nikov, *Izv. Akad. Nauk, Ser. Khim.*, 2009, 560 [*Russ. Chem. Bull.*, *Int. Ed.*, 2009, **58**, 572].
17. N. A. Sanina, N. S. Emel´yanova, A. N. Chekhlov, A. F. Shestakov, I. V. Sulimenkov, S. M. Aldoshin, *Izv. Akad. Nauk, Ser. Khim.*, 2010, 1104 [*Russ. Chem. Bull., Int. Ed.*, 2010, **59**, 1126].
18. C. L. Conrado, J. L. Baurossa, C. Egler, S. Wecksler, P. C. Ford, *Inorg. Chem.*, 2003, **42**, 2288.
19. X. Zhang, M. P. Broderick, *Mod. Asp. Immunobiol.*, 2000, **1**, No. 4, 160.
20. *Kratkii spravochnik khimika* [*Short Handbook of Chemistry*], Ed. V. I. Perel´man, Goskhimizdat, Moscow, 1963, 467 pp. (in Russian).
21. A. F. Dodonov, V. I. Kozlovski, I. V. Soulimenkov, V. V. Raznikov, A. V. Loboda, Z. Zhou, T. Horvath, H. Wollnik, *Eur. J. Mass Spectr.*, 2000, **6**, 481.

Received April 5, 2011;
in revised form August 4, 2011